

# Magnetic properties of arrays of nanowires: Anisotropy, interactions, and reversal modes

R. Lavin, J. C. Denardin, A. P. Espejo, A. Cortés, and H. Gómez

Citation: *Journal of Applied Physics* **107**, 09B504 (2010); doi: 10.1063/1.3350905

View online: <http://dx.doi.org/10.1063/1.3350905>

View Table of Contents: <http://aip.scitation.org/toc/jap/107/9>

Published by the [American Institute of Physics](#)

---

## Articles you may be interested in

### [Reversal modes in magnetic nanotubes](#)

*Applied Physics Letters* **90**, 102501 (2007); 10.1063/1.2437655

### [Angular dependence of magnetic properties in Ni nanowire arrays](#)

*Journal of Applied Physics* **106**, 103903 (2009); 10.1063/1.3257242

### [Angular dependence of the coercivity and remanence of ferromagnetic nanowire arrays](#)

*Journal of Applied Physics* **93**, 9202 (2003); 10.1063/1.1572197

### [Magnetic interactions and reversal mechanisms in Co nanowire and nanotube arrays](#)

*Journal of Applied Physics* **113**, 093907 (2013); 10.1063/1.4794335

### [The design and verification of MuMax3](#)

*AIP Advances* **4**, 107133 (2014); 10.1063/1.4899186

### [Magnetization mechanisms in ordered arrays of polycrystalline Fe<sub>100-x</sub>Co<sub>x</sub> nanowires](#)

*Journal of Applied Physics* **117**, 204302 (2015); 10.1063/1.4921701

---



## Instruments for Advanced Science

Contact Hiden Analytical for further details:

**W** [www.HidenAnalytical.com](http://www.HidenAnalytical.com)

**E** [info@hiden.co.uk](mailto:info@hiden.co.uk)

**CLICK TO VIEW** our product catalogue



### Gas Analysis

- › dynamic measurement of reaction gas streams
- › catalysis and thermal analysis
- › molecular beam studies
- › dissolved species probes
- › fermentation, environmental and ecological studies



### Surface Science

- › UHV TPD
- › SIMS
- › end point detection in ion beam etch
- › elemental imaging - surface mapping



### Plasma Diagnostics

- › plasma source characterization
- › etch and deposition process reaction
- › kinetic studies
- › analysis of neutral and radical species



### Vacuum Analysis

- › partial pressure measurement and control of process gases
- › reactive sputter process control
- › vacuum diagnostics
- › vacuum coating process monitoring

# Magnetic properties of arrays of nanowires: Anisotropy, interactions, and reversal modes

R. Lavin,<sup>1,2,3</sup> J. C. Denardin,<sup>1,3,a)</sup> A. P. Espejo,<sup>1</sup> A. Cortés,<sup>4</sup> and H. Gómez<sup>5</sup>

<sup>1</sup>Departamento de Física, Universidad de Santiago de Chile (USACH), Av. Ecuador 3493, Santiago 9170124, Chile

<sup>2</sup>Facultad de Ingeniería, Universidad Diego Portales, Ejército 441, Santiago 8370191, Chile

<sup>3</sup>Centro para el Desarrollo de la Nanociencia y Nanotecnología (CEDENNA), Av. Ecuador 3493, Santiago 9170124, Chile

<sup>4</sup>Departamento de Física, Universidad Técnica Federico Santa María, Av. España 1680, Casilla 110 V, Valparaíso 2390123, Chile

<sup>5</sup>Instituto de Química, Facultad de Ciencias, Pontificia Universidad Católica de Valparaíso, Casilla 4059, Valparaíso 2340025, Chile

(Presented 19 January 2010; received 6 November 2009; accepted 18 January 2010; published online 19 April 2010)

Arrays of Co and Ni nanowires of different lengths have been prepared by electrodeposition into nanopores of alumina membranes. The dependence of the coercivity of the arrays as a function of temperature and measurement angle of the nanowires has been measured. A simple model is presented in order to explain the behavior of the magnetic properties as a function of the angle of measurement. The analytical calculations show that while for Ni nanowires demagnetization reversal in the array is driven by means of the nucleation and propagation of a transverse wall, in Co arrays the reversal mode changes from curling to coherent when the angle of measurements changes. © 2010 American Institute of Physics. [doi:10.1063/1.3350905]

## I. INTRODUCTION

The research of magnetic nanostructures has gained a renewed interest with the development of the techniques for preparation of highly ordered arrays of magnetic nanowires inside nanopores of alumina membranes.<sup>1-4</sup> Technological applications are advised mainly in the high-density information storage.<sup>5,6</sup> Different groups have investigated the role of magnetostatic interactions and the influence of the size of nanowires on the magnetic properties of these systems.<sup>7-9</sup> However, for applications in magnetic recording devices, it is important to investigate in detail how the magnetic properties are affected when the magnetic field makes an angle with the nanowire axis. The properties of virtually all magnetic materials are controlled by domains separated by domain walls, and the way these domains reverse their magnetization in nanowires is determinant in the overall magnetic properties. The magnetization reversal in a magnetic nanowire, that is, the change in the magnetization from one of its minima ( $M_0\hat{z}$ ) to the other ( $-M_0\hat{z}$ ), may occur by means of three main idealized modes of magnetization reversal process that have been identified depending on the geometry and the composition of the wires.<sup>8,10,11</sup> These modes are known as the *coherent rotation*, C, with all the spins rotating simultaneously; *transverse wall*, T, in which spins invert progressively via propagation of a transverse domain wall; and the *vortex wall*, V, in which spins invert progressively via propagation of a vortex (curling) domain wall. The Stoner-Wohlfarth model has been applied to calculate the angular dependence of the coercivity when the reversal of magnetization is driven by coherent rotation.<sup>12</sup> On the other side, Aharoni<sup>13</sup> calculated the angular dependence of the nucle-

ation field when the reversal is driven by curling rotation. Recently Lavin *et al.*<sup>14</sup> calculated the angular dependence of the coercivity when the reversal of magnetization is driven by a transverse wall in Ni nanowire arrays. In this paper we present an analytical model that allows us to investigate the angular dependence of the coercivity for Ni and Co nanowire arrays, considering the different modes that can be present, as a function of wire geometry. Additionally, the magnetic properties in function of the temperature have been investigated in Ni and Co nanowire arrays in order to understand the effects of temperature and anisotropy of samples.

## II. EXPERIMENTAL METHODS

Hexagonal arrays of Ni and Co nanowires of diameters  $d=2R=50$  nm and different lengths have been prepared by

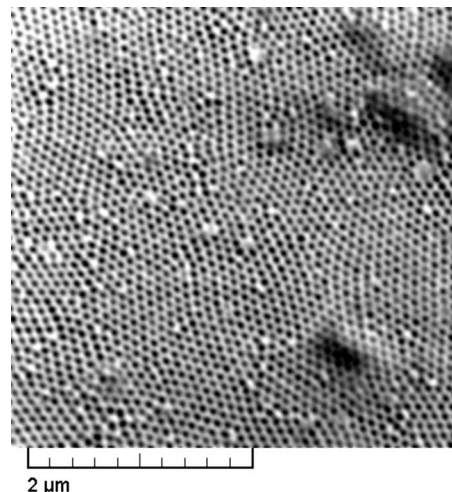


FIG. 1. SEM top view of a highly ordered homemade alumina template.

a)Electronic mail: jcdenardin@gmail.com.

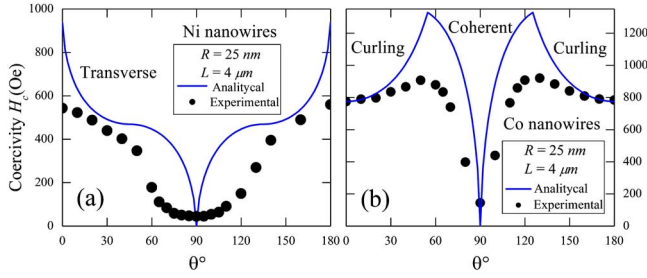


FIG. 2. (Color online) Angular dependence of the coercivity for arrays of (a) Ni and (b) Co nanowires with 50 nm of diameter. The black dots correspond to experimental data and the solid line represents the values calculated analytically.

electrodeposition into nanopores of alumina membranes with inter pore distance  $D=100$  nm,<sup>7</sup> see Fig. 1. The morphology of the individual nanowires after the dissolution of the alumina was studied by means of scanning electron microscopy (SEM) with a JEOL 5900 LV and transmission electron microscopy using a JEOL 2010F, checking the high ordering of the hexagonal arrays and the large aspect ratio.<sup>7</sup> The chemical characterization of the nanowires was made by means of energy-dispersive analysis of x-rays (Ref. 7) and x-ray diffraction.<sup>15</sup> The angular dependence of magnetization measurements was performed with vibrating sample magnetometer with the applied field at different angles between the external field and the nanowire axis. Measurements at low temperatures were performed in a Quantum Design MPMS system.

### III. RESULTS AND DISCUSSION

#### A. Reversal modes and interaction

In order to analyze our results for the angular dependence, we have developed analytical calculations that lead us to obtain the coercive field  $H_c^k$  for each of the reversal mechanisms,  $k=C, T$ , and  $V$ . The angular dependence of the nucleation for a C mode was calculated by Stoner–Wohlfarth<sup>12</sup> and gives

$$\frac{H_n^C(\theta)}{M_0} = -\frac{1 - 3N_z(L)}{2} \frac{\sqrt{1 - t^2 + t^4}}{1 + t^2},$$

where  $t = \tan^{1/3}(\theta)$  and  $M_0$  is the saturation of magnetization. The demagnetizing factor of a wire along the  $z$  axis has been previously obtained<sup>16,17</sup> and is given by  $N_z(L) = 1 - F_{21}[4R^2/L^2] + 8R/3\pi L$ , where  $F_{21}[x] = F_{21}[-1/2, 1/2, 2, -x]$  is a hypergeometric function and  $L$  is the length of nanowire.

The angular dependence of the coercivity for a T mode can be studied by an adapted Stoner–Wohlfarth model in which the width of the domain wall  $\omega_T$  is used as the length of the region undergoing coherent rotation.<sup>14,16,17</sup> Starting from the equation presented by Landeros *et al.*<sup>11</sup> we calculate the width of the domain wall for the transverse mode as a function of the wire geometry.<sup>7</sup> Following this approach,

$$\frac{H_n^T(\theta)}{M_0} = -\frac{1 - 3N_z(\omega_T)}{2} \frac{\sqrt{1 - t^2 + t^4}}{1 + t^2}.$$

As shown in the Stoner–Wohlfarth model,<sup>12</sup> the nucleation field does not represent the coercivity in all cases. However,

from the discussion in p. 21 of Ref. 13, the coercivity can be written as

$$H_n^{C,T}(\theta) = \begin{cases} |H_n^{C,T}| & 0 \leq \theta \leq \pi/4 \\ 2|H_n^{C,T}(\theta = \pi/4)| - |H_n^{C,T}| & \pi/4 \leq \theta \leq \pi/2 \end{cases}.$$

The angular dependence of the vortex (curling) nucleation field in a finite prolate spheroid was obtained by Aharoni,<sup>13</sup>

$$\frac{H_n^V}{M_0} = \frac{\left(N_z - \frac{q^2 L_x^2}{R^2}\right) \left(N_x - \frac{q^2 L_x^2}{R^2}\right)}{\sqrt{\left(N_z - \frac{q^2 L_x^2}{R^2}\right)^2 \sin^2 \theta + \left(N_x - \frac{q^2 L_x^2}{R^2}\right)^2 \cos^2 \theta}},$$

where  $L_x$  is the exchange length of the material and  $q^2 = 112/33$ . As was shown by Aharoni,<sup>13</sup> the coercivity of a spheroid is a good approximation for  $-H_n^V$ .

With the above expressions we can study the angular dependence of the coercivity for our arrays and explain the experimental difference observed for Ni and Co nanowires. In our model the system reverses its magnetization by the mode that first opens an energetically accessible route, that is, by the mode that exhibits the lowest coercivity. However, for highly dynamic cases, the path of lowest coercivity might not be accessible due to precession effects. By evaluating the coercivity for the different modes described above we found the one which drives the reversal for each  $\theta$ .

Figure 2 shows the angular dependence of the coercivity for arrays of Ni [Fig. 2(a)] and Co [Fig. 2(b)] nanowires with 50 nm of diameter. In the Ni nanowire arrays the transversal mode T is dominant in almost the entire angle interval  $\theta$ , because this transversal mode exhibits a lower coercivity.<sup>14</sup> The solid line in Fig. 2(a) is the calculated angular dependence of coercivity for the transversal reversion mode and follows the same tendency of the experimental points. On the other hand, for Co nanowire arrays there is a transition in the coercivity when the angle  $\theta = 55^\circ$ , as can be observed in the experimental results [dots in Fig. 2(b)]. The solid line in Fig. 2(b) is the result of the analytical model for  $H_c(\theta)$ , calculated with the vortex mode  $H_n^V$  for  $\theta < 56^\circ$ , and the coherent rotation mode  $H_n^C$  for  $\theta > 56^\circ$ . It is worth to note that the crossing point between the vortex and coherent mode in Co nanowires is the same for the experimental data and analytical result, and there is a very good agreement between the experimental and calculated coercivity values. The difference in the absolute values of coercivity in the calculated curves and the experimental data can be ascribed to size distribution and dipolar interactions between the nanowires, and was not considered so far in this model.

For arrays of Ni nanowires with vortex and transversal reversal modes it is possible to include the influence of the interactions between nanowires, analytically only for  $\theta = 0^\circ$  and  $90^\circ$ . A model that considers the interaction field in nanowire networks has been previously used to fit the angular dependence of ferromagnetic resonance fields in arrays of nanowires.<sup>18,19</sup> In a previous work<sup>7</sup> we have calculated the stray field produced by the array on one nanowire when the reversion of magnetization occurs in T mode, which occurs for nanowires with  $R < 30$  nm.<sup>11</sup> The coercive field in this case is given by  $H_c^T = H_c^i - H_{\text{int}}^T$ ,<sup>7</sup> where  $H_c^i$  denotes the intrinsic

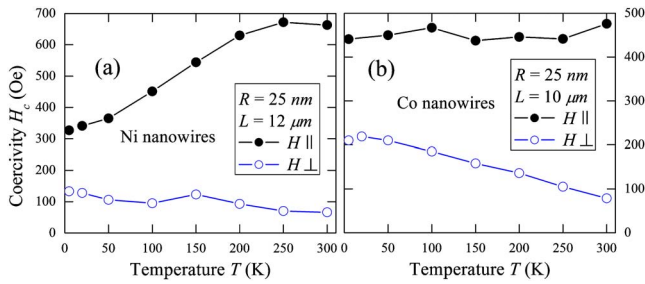


FIG. 3. (Color online) Temperature dependence of the coercivity for arrays of (a) Ni nanowires with length of 12  $\mu\text{m}$  and (b) Co with length of 10  $\mu\text{m}$  measured parallel and perpendicular to the wire axis.

sic coercivity of an isolated nanowire in T mode, and  $H_{\text{int}}$  corresponds to the stray field induced within the array given by  $H_{\text{int}} = [2K(L)/\mu_0 M_0][\epsilon|E_{\text{int}}|/K(L)]^{1/2}$  with  $K(L) = (1/4)\mu_0 M_0^2[1 - 3N_z(L)]$ , and  $E_{\text{int}}$  is the interaction field between two nanowires.<sup>7</sup> Using this approach, the coercivity calculated at  $\theta = 0^\circ$  for the array of Ni nanowires with  $R = 25$  nm and  $L = 4$   $\mu\text{m}$  gives coercivity values more close to the ones observed in the experimental points.

## B. Anisotropy and temperature

Figure 3 shows the temperature dependence of the coercivity for arrays of Ni nanowires with length of 12  $\mu\text{m}$  [Fig. 3(a)] and Co with length of 10  $\mu\text{m}$  [Fig. 3(b)], measured parallel and perpendicular to the wire axis. For the Ni array the coercivity measured parallel to the nanowires increases with the temperature and the coercivity measured perpendicular slightly decreases when the temperature increases. In Co nanowires the coercivity dependence with temperature is opposite to the Ni nanowires, as can be seen in Fig. 3(b). In order to explain these different dependences in Ni and Co one has to consider the contribution of the magnetocrystalline and magnetoelastic anisotropies. The crystalline anisotropy constant of Ni increases two orders of magnitude when temperature decreases from 300 to 5 K. The magnetoelastic anisotropy, on the other hand, depends on the stress applied to the wires by the alumina matrix and is affected by the different thermal expansion coefficients of the alumina porous and the nanowires.<sup>20,21</sup> A more systematic characterization of arrays of Ni, Co, and segmented Ni/Co nanowires measured at different angles and as function of temperature could help us to identify the different reversal modes that take place at different temperatures and understand better the complexity of the low temperature effects.

## IV. CONCLUSION

By means of experimental measurements and analytical calculations we have investigated the angular dependence of the magnetization in Ni and Co nanowire arrays. As found from experiments, the angular dependence in large aspect ratio wires can be understood assuming that the relaxation process is very fast and then the magnetization orients rapidly along the easy axes. We have derived analytical expressions that allow us to obtain the coercivity when the wire

reverses its magnetization by means of a coherent rotation, transverse reversal mode, and a vortex domain wall. For the Ni wires studied experimentally the magnetization is driven by means of the nucleation and propagation of a transverse wall, while for Co nanowires there is a transition between vortex and coherent rotation near  $\theta = 55^\circ$ . The stray field produced by the array, as a function of the angle of the external field, cannot be determined analytically. However, it is responsible for small differences between experiments and calculations. The temperature dependence of coercivity for Ni and Co arrays has been measured with the applied field parallel and perpendicular to the wires. The puzzling effect of the competition of the different anisotropies at low temperatures could be cleared out by a detailed study of the arrays at low temperature and as a function of angle of measurement.

## ACKNOWLEDGMENTS

This work was supported by the Proyecto Fondecyt Postdoctorado (Grant No. 3100117), the Financiamiento Basal para Centros Científicos y Tecnológicos de Excelencia (CEDENNA), the Millennium Science Nucleus Basic and Applied Magnetism (Grant No. P06-022F), and the Fondecyt (Grant Nos. 1080164 and 3080058).

- <sup>1</sup>H. Masuda and K. Fukuda, *Science* **268**, 1466 (1995).
- <sup>2</sup>K. Nielsch, R. B. Wehrspohn, J. Barthel, J. Kirschner, U. Gosele, S. F. Fischer, and H. Kronmüller, *Appl. Phys. Lett.* **79**, 1360 (2001).
- <sup>3</sup>Z. K. Wang, H. S. Lim, V. L. Zhang, J. L. Goh, S. C. Ng, M. H. Kuok, H. L. Su, and S. L. Tang, *Nano Lett.* **6**, 1083 (2006).
- <sup>4</sup>J. Escrig, D. Altbir, M. Jaafar, D. Navas, A. Asenjo, and M. Vazquez, *Phys. Rev. B* **75**, 184429 (2007).
- <sup>5</sup>S. A. Wolf, D. D. Awschalom, R. A. Buhrman, J. M. Daughton, S. von Molnar, M. L. Roukes, A. Y. Chtchelkanova, and M. Treger, *Science* **294**, 1488 (2001).
- <sup>6</sup>Th. Gerrits, H. A. M. van der Berg, J. Hohlfield, L. Bar, and Th. Rasing, *Nature (London)* **418**, 509 (2002).
- <sup>7</sup>J. Escrig, R. Lavin, J. L. Palma, J. C. Denardin, D. Altbir, A. Cortes, and H. Gomez, *Nanotechnology* **19**, 075713 (2008).
- <sup>8</sup>R. Hertel, *J. Magn. Magn. Mater.* **249**, 251 (2002).
- <sup>9</sup>R. Lavin, J. C. Denardin, J. Escrig, D. Altbir, A. Cortes, and H. Gomez, *IEEE Trans. Magn.* **44**, 2808 (2008).
- <sup>10</sup>H. Forster, T. Schrefl, W. Scholz, D. Suess, V. Tsiantos, and J. Fidler, *J. Magn. Magn. Mater.* **249**, 181 (2002).
- <sup>11</sup>P. Landeros, S. Allende, J. Escrig, E. Salcedo, D. Altbir, and E. E. Vogel, *Appl. Phys. Lett.* **90**, 102501 (2007).
- <sup>12</sup>E. C. Stoner and E. P. Wohlfarth, *Philos. Trans. R. Soc. London, Ser. A* **240**, 599 (1948).
- <sup>13</sup>A. Aharoni, *J. Appl. Phys.* **82**, 1281 (1997).
- <sup>14</sup>R. Lavin, J. C. Denardin, J. Escrig, D. Altbir, A. Cortes, and H. Gomez, *J. Appl. Phys.* **106**, 103903 (2009).
- <sup>15</sup>A. Cortés, G. Riveros, J. L. Palma, J. C. Denardin, R. E. Marotti, E. A. Dalchiale, and H. Gómez, *J. Nanosci. Nanotechnol.* **9**, 1992 (2009).
- <sup>16</sup>J. Escrig, M. Daub, P. Landeros, K. Nielsch, and D. Altbir, *Nanotechnology* **18**, 445706 (2007).
- <sup>17</sup>S. Allende, J. Escrig, D. Altbir, E. Salcedo, and M. Bahiana, *Eur. Phys. J. B* **66**, 37 (2008).
- <sup>18</sup>I. Dumitru, F. Li, J. B. Wiley, D. Cimpoesu, A. Stancu, and L. Spinu, *IEEE Trans. Magn.* **41**, 3361 (2005).
- <sup>19</sup>O. C. Trusca, D. Cimpoesu, J. H. Lim, X. Zhang, J. B. Wiley, A. Diaconu, I. Dumitru, A. Stancu, and L. Spinu, *IEEE Trans. Magn.* **44**, 2730 (2008).
- <sup>20</sup>A. Kumar, S. Fahler, H. Schlorb, K. Leistner, and L. Schultz, *Phys. Rev. B* **73**, 064421 (2006).
- <sup>21</sup>E. L. Silva, W. C. Nunes, M. Knobel, J. C. Denardin, D. Zanchet, K. Pirotta, D. Navas, and M. Vazquez, *Physica B* **384**, 22 (2006).